JAYCOR

Response to NRC Request For Additional Information

HADDAM NECK

Re: Licensee Response to Bulletin 88-02

JAYCOR Report J1681-91-001R0

June 1991

Prepared by

JAYCOR
9775 Towne Center Drive
San Diego, California 92121-1996

Principal Investigator

P. J. Masiello

Prepared for

S. Chandra

Northeast Utilities Service Company
Berlin, Connecticut

9775 Towne Centre Drive • San Diego, California 92121 • (619) 453-6580
Post Office Box 85154 • San Diego, California 92186-5154 • FAX (619) 452-7899

Contents

Illustrations

Tables

Summary

In this report, information is supplied to the NRC in response to their review of a fluidelastic instability analysis performed for the Westinghouse Model 27 steam generator, on behalf of Northeast Utilities Service Company (NUSCO). Westinghouse Model 27 steam generators have been operational since 1967 at the Connecticut Yankee nuclear power plant at Haddam Neck.

A fluidelastic instability analysis of the Westinghouse Model 27 was performed by JAYCOR, San Diego, in 1989 as part of a program plan initiated by NUSCO in response to NRC Bulletin No. 88-02, relevant to the North Anna 1 tube rupture incident (July 1987). In the present report, follow-up information is presented in connection with six questions posed in the NRC review of the JAYCOR paper "Fluidelastic Instability Analysis of the U-Bend region of a Westinghouse Model 27 Steam Generator," J5439-89-001, June 1989.

The response to the NRC review includes a comparison of the maximum susceptibility ratios, predicted for the Westinghouse Model 27 with those determined by the same method for the Westinghouse Model 51 with operational parameters and geometric specifications characteristic of those for North Anna 1 at the time of the tube rupture. Hence, the JAYCOR model for evaluating fluidelastic instability is qualified with data applicable to a known tube failure. The result of the benchmark comparison showed that for North Anna 1, the JAYCOR model did indeed predict susceptibility ratios, S, exceeding 1.0, the conventionally accepted value above which a fluidelastic instability can occur. The model predictions also indicated that values of $S > 1.0$ (e.g., as large as 1.464) occurred at locations within the spatial resolution applicable to the thermal-hydraulic calculation (three tube pitches), of the failed North Anna tube, R9C51. Susceptibility ratios predicted for the Model 27 were typically smaller than 0.65, with a maximum value of $S = 0.88$ near the bundle periphery, where flow peaking is not expected to play a significant role.

In the subject evaluation, the net resultant velocity vector in cross-flow with tubes, consisting of components in the plane of the U-tubes and normal to this plane, were employed for analyses of the Westinghouse Model 27 at Haddam Neck, and the Model 51 at North Anna. Damping coefficients which are input parameters to the fluidelastic instability analyses were deduced from the same empirical damping curve for steam-water mixtures (Axisa, 1988), in a consistent manner for both evaluations.

It is felt that the analysis for the Westinghouse Model 27 steam generators at Haddam Neck is conservatively based, since the ATHOS3 thermal-hydraulic simulation corresponded to a circulation ratio of $CR = 4.54$, and the actual circulation ratio could be as low as 3.8. A lower circulation ratio would indicate that the flow rate through the wrapper region is reduced proportionally, and consequently, the local velocities in the U-bend region would be smaller than predicted. In light of this conservative approach, and due to the smaller susceptibility ratios predicted for the Model 27, corrective action (e.g., downcomer flow restriction or tube plugging) is not deemed necessary for the Haddam Neck plant.

Introduction

The objective of the present report is to provide the NRC with requested information and results of additional fluidelastic instability analyses performed in connection with their review of an earlier paper, "Fluidelastic Instability Analysis of the U-Bend region of a Westinghouse Model 27 Steam Generator," JAYCOR Report J5439-89-001, June 1989. The JAYCOR paper was presented to the NRC on behalf of Northeast Utilities Service Company, in response to NRC Bulletin No. 88-02, "Rapidly Propagating Fatigue Cracks in Steam Generator Tubes," February 1988. The failure of a U-tube on the cold leg of a Westinghouse Model 51 steam generator at the North Anna plant (Virginia Power Company) in July of 1987 brought about renewed interest in the possibility of a tube rupture in similar Westinghouse designs. The more recent incident in February of 1991 at Mihama-2 at the Kansai Electric nuclear power plant in Japan, presents itself as another example of a similar type of failure.

The 1989 JAYCOR analysis which relates to Bulletin 88-02 found that no corrective action was required for safe operation of the Westinghouse Model 27 steam generators at Haddam Neck. This result was in keeping with a conventionally accepted upper bound of susceptibility ratio of 1.0, corresponding to the onset of fluidelastic instability. At the request of the NRC, the JAYCOR model has been qualified in the present study by means of a similar evaluation of fluidelastic instability for the known failed tube, R9C51, at North Anna 1.

In their review of the original JAYCOR analysis, the NRC posed six questions, which are addressed in sequence in the present report, in Sections 1 through 6, respectively. Of special importance is Section 1, which describes results of an evaluation of North Anna 1, thus qualifying the JAYCOR model with a known failed tube, and establishing a quantitative measure of the susceptibility ratio for the onset of instability. Also noteworthy is Section 5, where justification is presented for the selection of the damping ratio employed in the JAYCOR fluidelastic instability analyses of the Westinghouse Model 27 and 51 steam generators.

A general discussion is presented in Section 7, which includes responses to relevant comments made by the NRC during a joint NRC/NUSCO/JAYCOR conference call which took place on April 26, 1991.

1. Response to NRC Item 1: North Anna Model Validation

In accordance with the NRC request to evaluate the fluidelastic instability of the failed tube R9C51 of North Anna, a study was made in which all tube columns of five rows surrounding and including R9C51 were analyzed with methods identical to those described in Reference 1.

Since we were not provided with operational and geometric input data corresponding to North Anna Unit 1 at the time of failure in July of 1987, we have assumed the task of compiling data we feel should reflect North Anna. The source of the data base we assembled is essentially information we have received from EPRI and Westinghouse over the last decade, while engaged in a number of EPRI funded projects relating to steam generator technology. JAYCOR has served as consultants to Westinghouse on several occasions, and we have had a proprietary data disclosure agreement with them. We are quite confident in the geometric data which we have employed for the Model 51 steam generator at North Anna. The operational parameters (e.g., dome pressure, feedwater mass flow rate, etc.) we have assumed are design values for the North Anna plant at 100% load. The dome pressure value we employed reflects the actual secondary fluid overpressure for North Anna 1 at the time of failure. We feel that any discrepancies between our overall data set and actual North Anna conditions would be very minor, and would not affect the outcome of our study. The operational data and geometric specifications assumed for the Westinghouse Model 51 at North Anna 1 are provided in Tables 1-1 and 1-2, respectively.

The set of tubes evaluated for North Anna comprises rows 7 through 11, U-tubes with the largest bend radii which might be unsupported by antivibration bars (AVB's). The design criterion for the Model 51 was to provide AVB support to all rows beyond row 10. Inspections have shown, however, that this design objective was not met or was exceeded for many rows. Bend radii which are larger relative to others result in lower natural frequencies and lower critical velocities, which would be detrimental to fluidelastic instability. Thus, it is of most interest to consider tubes with the largest bend radii which might be unsupported by AVB's. The failed tube, row 9 column 51 (R9C51) of North Anna is a member of the group evaluated for instability, and is of primary interest, serving as a benchmark for model validation.

The overall method for assessing fluidelastic instability for North Anna is identical to that reported in Reference 1. It consists of three steps:

[1] Thermal-hydraulic simulation of two-phase three-dimensional flow using the ATHOS3 steam generator code.

[2] Modal analyses of the U-tube section above the uppermost tube support plate by means of the ADINA finite element code.

[3] Post-processing of data from the ATHOS3 solution and from modal analyses by ADINA, to arrive at susceptibility ratios for the dominant modes of vibration.

Table 1-1. Operating Parameters Assumed for Westinghouse Model 51 Steam Generator at North Anna 1

Dome pressure	890 psia
Feedwater mass flow rate/SG	4.26×10^6 lb/hr
Feedwater temperature	440°F
Primary flow rate/SG	32.97×10^6 lb/hr
Primary inlet temperature	621.0°F
Primary outlet temperature	552.0°F
Primary pressure	2250 psia
Exit steam quality	0.9975
Carryunder	0.0025
Height above tube sheet of water level water level in downcomer	505.9 in.
Circulation ratio	4.6

1.1 THERMAL-HYDRAULIC SIMULATION

With regard to Step [1], we have employed an identical finite-difference grid, a $26(\theta) \times 12(r) \times 35(z)$, consisting of 10,920 active cells (Figures 3-1 and 3-2 of Reference 1). Since the dimensions of the Model 51 steam generator are distinct from those of the Model 27 at Haddam Neck, the axial slab positioning had to be altered for North Anna. However, the number of axial cells allocated to the U-bend region, 14, was kept the same as for the Model 27, resulting in the same spatial resolution of about three cell pitches per axial cell. This is considered fine resolution for an ATHOS3 simulation. The grid in the r-θ plane was identical to that in the Model 27 study (Figure 3-1 of Reference 1), with radial nodes scaled up linearly to the Model 51 wrapper radius.

Since we were not provided with detailed geometric information regarding the AVB configuration for the Model 51, we were not able to account for the presence of AVB's in the ATHOS3 thermal-hydraulic simulation. Since AVB's (and their nonuniform penetration depths) were at least partially accounted for in the Westinghouse Model 27 analysis, this can be interpreted as conservative in the following sense. If an assessment is made of the stability of Model 27 U-tubes, the susceptibility ratios for the Model 27 analysis would be biased to the high side relative to those for the known failed tube of the Model 51, since some finite flow peaking effects would be calculated for Haddam Neck and not for North Anna.

The ATHOS3 calculation of the Model 51 converged to steady-state in 460 iterations ("sweeps"), with maximum cycle-to-cycle pressure correction less than 5 Pa. The predicted values of circulation ratio and primary inlet temperature of 4.719 and 602.9°K, respectively, agree well with design values (4.6 and 600.5°K, respectively) for North Anna at full power conditions. The good agreement of circulation ratio implies that the code predicted a representative amount of

Table 1-2. Geometric Specification of Westinghouse Model 51 Steam Generator at North Anna 1

All heights are referenced to top of tube sheet

1. Shell and Wrapper	
Internal diameter of lower part of shell	129.38 in.
Internal diameter of upper part of shell	168.50 in.
Starting elevation of shell expansion	353.13 in.
Ending elevation of shell expansion	431.36 in.
Internal diameter of lower part of wrapper	123.75 in.
Internal diameter of upper part of wrapper	135.12 in.
Starting elevation of wrapper expansion	394.31 in.
Ending elevation of wrapper expansion	417.02 in.
Wrapper thickness	0.38 in.
Starting elevation of wrapper wall	14.00 in.
2. Tube Bundle	
Outer diameter of tubes	0.875 in.
Inner diameter of tubes	0.775 in.
Tube pitch	1.281 in.
Pitch type	square
Starting elevation of U-bend region	356.45 in.
Ending elevation of U-bend region	416.72 in.
Distance between centerline of first row of tubes and tube lane axis	2.190 in.
Number of tube rows	46
Number of tube columns	94
Total number of tubes	3388
Largest U-bend radius	59.83 in.
Smallest U-bend radius	2.19 in.
Total heat transfer area of bundle	51,495 ft^2
Tube material	Inconel 600
Thickness of tube sheet	21.44 in.
3. Tube Support Plates	
Number of tube support plates	7
Elevations of tube support plates: (to center of plate thickness)	
Plate #1:	50.125 in.
Plate #2:	100.625 in.

Table 1-2. Cont'd.

3. Tube Support Plates (Cont'd)

Plate #3:	151.125 in.
Plate #4:	201.625 in.
Plate #5:	252.125 in.
Plate #6:	302.625 in.
Plate #7:	353.125 in.
Radial extent of tube support plates	61.875 in.
Tube support plate metal area density (ratio of plate metal area to nominal geometric cross-sectional area)	0.33904

flow through the wrapper interior (e.g., U-bend region). The three-dimensional distribution of void fraction and secondary fluid velocity predicted by ATHOS3 was saved in a permanent file for post-processing.

1.2 MODAL ANALYSES

The first four dominant modes of vibration were calculated by the ADINA structural analysis code, for the sections of tube rows 7 through 11 above the uppermost support plate. This includes a short straight section (about 3 inches) joined by an inverted semicircle of bend radius varying from 9.9 inches for row 7 to 15.0 inches for row 11. A total of 41 finite element nodes were employed along each tube, as for the Model 27 analyses. (The nodal layout is shown in Figure 5-1 of Reference 1). The boundary condition is assumed to be a fully clamped rigid support, since denting is assumed at the topmost support plate. The natural frequencies of the first four dominant modes for rows 7 through 11 are shown in Table 1-3 for the ADINA calculations. The fundamental mode of each tube was again found to be an out-of-plane symmetric flexure in which all nodes move in the same direction. The maximum deflection occurs at the apex of each tube.

A comparison of natural frequencies in Table 1-3 with those of Table 5-3, Reference 1, indicates that the dominant frequency of a Model 51 tube is about 30% higher than for a Model 27 tube of an equivalent bend radius (e.g., 79 Hz for row 8 of Model 51 vs. 60 Hz for row 10 of Model 27). This is attributable mostly to the increase in tube diameter for the Model 51 (0.875 in. vs. 0.750 in.), and to the decrease in the straight stub length as well. For a thin walled tube, the natural frequency is roughly proportional to the tube diameter raised to the 3/2 power. The increase in the dominant frequencies is favorable to the goal of avoiding a fluidelastic instability, since the critical velocities will be higher. However, other factors must also be considered, as will become evident later.

Table 1-3. Natural Frequencies of First Four Dominant Modes of Vibration for Model 51 at North Anna 1.

Row	R in.	f_1 Hz	f_2 Hz	f_3 Hz	f_4 Hz
7	9.876	96.59	215.4	271.9	506.2
8	11.157	78.87	177.4	222.8	413.5
9	12.438	65.61	148.7	185.9	344.2
10	13.719	55.43	126.4	157.4	291.3
11	15.000	47.44	108.7	134.9	249.3

1.3 POST-PROCESSING

A fluidelastic instability analysis was performed for the North Anna U-tubes of interest, utilizing two-phase flow thermal-hydraulic data predicted by ATHOS3 and modal displacement and natural frequency data from the ADINA code. Susceptibility ratios, defined as ratios of effective velocity to the critical velocity, were evaluated for all columns of the five rows examined. The critical velocity is defined by Conners' equation,

$$V_{crit} = KfD_o \left[\frac{2\pi\, m_e\, \zeta}{\rho_e D_o^2}\right]^{1/2} \qquad (1)$$

where

K = Conners' coefficient, taken as 3.3

f = natural frequency of tube, Hz

D_o = tube outer diameter

m_e = effective mass per unit tube length

ζ = total damping ratio

ρ_e = effective secondary fluid density.

The value of K = 3.3 was retained from the earlier study of the Model 27 [1], since it appears to have wide acceptance in the literature [2, 3, 4, 5] as a conservative value for flow in steam

generators. Conners' coefficient may be a function of pitch-to-diameter ratio ("confinement"), and higher values of K have been reported, but generally there is a scarcity of available experimental data for two-phase flow, particularly steam-water.

The selection of a suitable value for the total damping ratio, ζ, is not so straightforward. For further details, see the response to NRC Item 5 presented in Section 5. Here, it should suffice to mention that we have employed an empirical curve of total damping versus void fraction, shown in Figure 1-1 (Figure 17 of Reference 2), taken from data measured by Axisa [6] for steam-water two-phase flow at 210°C. In conjunction with Figure 1-1 we have used an average value of void fraction applicable to the three-dimensional space occupied by the ensemble of tubes of interest (rows 7-11 of the Model 51) in the U-bend region, taken from the ATHOS3 code prediction. For the Model 51 calculation, the appropriate value of average void is $\alpha_{avg} = 0.86$. This average void pertains to the group of tubes examined, and may differ from the average value for the entire U-bend region. The associated value of total damping is obtained from Figure 1-1 as $\zeta = 0.017$, applicable to our North Anna evaluation.

The selection of a suitable effective cross-flow velocity is also not straightforward for curved tubes in the U-bend region. It has not yet been shown that methods of estimating the effective velocity for a straight tube are directly applicable to tubes with curvature. One complication is that there are velocity components normal to the tubes which are both in the plane of the tube and out-of-plane. In accordance with the preference of the NRC (see Section 6), we have calculated the resultant of the in-plane and out-of-plane cross-flow velocity components for a given tube. A tube gap velocity is deduced from the code velocity for the two-fluid mixture, in each coordinate direction, and employed in the calculation of effective cross-flow velocity by integration of interpolated values along the finite element nodes of a tube.

1.4 RESULTS OF FLUIDELASTIC INSTABILITY ANALYSES FOR MODELS 27 AND 51

1.4.1 Model 27

Our original evaluation (Ref. 1) of the Westinghouse Model 27 steam generators at Haddam Neck employed the out-of-plane component of tube gap velocity in the determination of effective velocity. We have since then repeated our analyses using the magnitude of the resultant of the in-plane and out-of-plane tube gap velocity vectors, as described above. Simultaneously, we have modified the value of total damping to be consistent with the practice we adopted for the determination of ζ for the Model 51, as described earlier. The average value of void fraction predicted by ATHOS3 in the region occupying tube rows 12 through 16 of the Model 27 U-bend region is $\alpha_{avg} = 0.74$. The corresponding value of total damping inferred from the steam-water curve of Figure 1-1 is $\zeta = 0.025$, slightly lower than the value of $\zeta = 0.030$ employed in the original study [1]. Conners' coefficient (K = 3.3), and other parameters in Eq. 1 remain unchanged from the original evaluation.

Resulting values of susceptibility ratio V_{eff}/V_{crit} for tube rows 10, 12 and 14 of the Model 27 are shown in Tables 1-4, 1-5 and 1-6, respectively. It should be noted here that in Tables 1-4

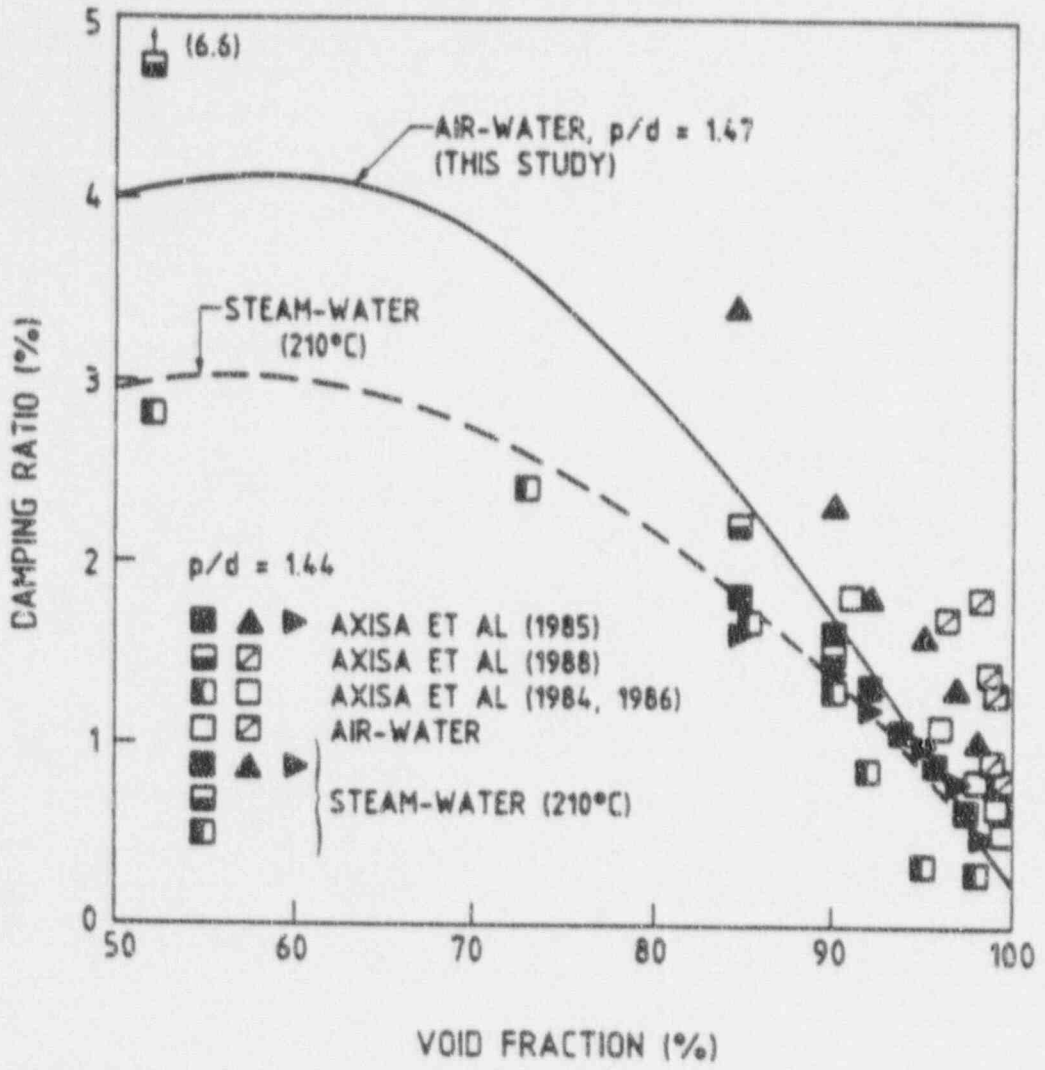

Figure 1-1. Damping of tube bundles in two-phase cross-flow: Comparison with results of Axisa [6] for steam-water. Normal square: □; parallel triangular: △; normal triangular: ▷. Reprinted from Reference 6, Pettigrew, Taylor and Kim.

Table 1-4. Westinghouse Model 27 Steam Generator.

Fluidelastic Instability Analysis of Row 10, Bend Radius = 11.154 in.

Column	Me kg/m	Rho kg/m**3	Veff m/sec	Vcrit m/sec	Veff/Vcrit
51	0.83987	156.518	3.231	5.756	0.561
52	0.83967	156.333	3.167	5.759	0.550
53	0.83872	154.343	3.071	5.793	0.530
54	0.83806	152.780	3.006	5.820	0.517
55	0.83774	151.914	3.018	5.835	0.517
56	0.83755	151.367	3.015	5.845	0.516
57	0.83742	150.992	3.009	5.852	0.514
58	0.83745	150.999	3.016	5.852	0.515
59	0.83760	151.358	3.028	5.846	0.518
60	0.83815	152.636	2.994	5.823	0.514
61	0.83881	154.195	2.965	5.796	0.512
62	0.83936	155.540	2.900	5.772	0.502
63	0.84001	157.020	2.831	5.747	0.493
64	0.84048	157.976	2.809	5.732	0.490
65	0.84082	158.717	2.778	5.719	0.485
66	0.84109	159.375	2.756	5.708	0.483
68	0.84126	160.048	2.729	5.697	0.479
69	0.84044	158.272	2.698	5.726	0.471
70	0.83935	155.921	2.686	5.765	0.466
73	0.83618	149.452	2.708	5.878	0.461
74	0.83526	147.675	2.714	5.910	0.459
80	0.83790	152.236	2.685	5.830	0.461
81	0.83857	153.557	2.687	5.807	0.463
82	0.83932	155.068	2.685	5.781	0.464
83	0.84030	157.132	2.698	5.746	0.469
84	0.84149	159.705	2.710	5.704	0.475
85	0.84278	162.443	2.715	5.666	0.480
86	0.84423	165.549	2.722	5.611	0.485
87	0.84573	168.850	2.728	5.561	0.491
88	0.84702	171.720	2.732	5.519	0.495
89	0.84780	173.390	2.725	5.495	0.496
92	0.85103	180.498	2.706	5.396	0.502
93	0.85259	184.020	2.699	5.349	0.505
94	0.85447	188.273	2.703	5.294	0.511
95	0.85979	200.352	2.986	5.149	0.564
96	0.86662	215.813	3.197	4.979	0.642
97	0.87350	231.375	3.469	4.828	0.719
98	0.88040	247.033	3.746	4.691	0.798
99	0.88664	261.232	4.010	4.578	0.878

Statistics for row 10 with natural frequency 60.08 hz:

Average value of Veff/Vcrit = 0.524 over all tube columns processed
Maximum value of Veff/Vcrit = 0.878 occurs at tube column 99

Table 1-5. Westinghouse Model 27 Steam Generator.

Fluidelastic Instability Analysis of Row 12, Bend Radius = 13.216 in.

Column	Me kg/m	Rho kg/m**3	Veff m/sec	Vcrit m/sec	Veff/Vcrit
51	0.83777	151.678	3.220	4.456	0.723
52	0.83768	151.706	3.172	4.455	0.712
53	0.83662	149.413	3.042	4.486	0.678
54	0.83619	148.402	3.005	4.500	0.668
55	0.83568	147.160	2.965	4.518	0.656
56	0.83575	147.198	2.997	4.518	0.664
57	0.83574	147.113	2.994	4.519	0.663
58	0.83582	147.267	2.992	4.517	0.663
59	0.83607	147.858	3.006	4.508	0.667
60	0.83639	148.653	3.013	4.497	0.670
61	0.83686	149.799	2.993	4.481	0.668
62	0.83745	151.139	2.937	4.463	0.658
63	0.83812	152.643	2.888	4.443	0.650
64	0.83879	154.082	2.828	4.424	0.639
65	0.83947	155.585	2.795	4.404	0.635
66	0.84015	157.121	2.782	4.384	0.635
67	0.84064	158.266	2.769	4.369	0.634
68	0.84062	158.652	2.735	4.365	0.627
69	0.84061	157.886	2.736	4.374	0.624
70	0.83943	155.640	2.738	4.404	0.622
71	0.83834	153.220	2.745	4.435	0.619
72	0.83713	150.704	2.741	4.468	0.613
73	0.83587	148.175	2.753	4.503	0.611
74	0.83465	145.826	2.755	4.536	0.607
75	0.83447	145.361	2.749	4.543	0.605
76	0.83432	144.901	2.750	4.548	0.605
77	0.83424	144.751	2.745	4.551	0.603
78	0.83432	144.882	2.740	4.550	0.602
79	0.83459	145.357	2.737	4.543	0.603
80	0.83514	146.380	2.742	4.529	0.606
81	0.83576	147.612	2.750	4.511	0.610
82	0.83637	148.793	2.748	4.495	0.611
83	0.83726	150.570	2.752	4.471	0.615
84	0.83838	152.723	2.757	4.442	0.621
85	0.83960	155.466	2.768	4.406	0.628
86	0.84110	158.654	2.770	4.365	0.635
87	0.84260	161.987	2.767	4.325	0.640
88	0.84394	164.869	2.771	4.289	0.646
89	0.84491	166.958	2.768	4.265	0.649
90	0.84588	169.051	2.764	4.243	0.651
91	0.84687	171.202	2.762	4.217	0.653
92	0.84841	174.626	2.762	4.179	0.658
93	0.85003	178.245	2.748	4.140	0.664
94	0.85231	183.432	2.776	4.087	0.679
95	0.85796	196.257	3.019	3.964	0.761
96	0.86497	212.097	3.339	3.829	0.872

Statistics for row 12 with natural frequency 45.84 hz:

Average value of Veff/Vcrit = 0.648 over all tube columns processed
Maximum value of Veff/Vcrit = 0.872 occurs at tube column 96

Table 1-6. Westinghouse Model 27 Steam Generator.

Fluidelastic Instability Analysis of Row 14, Bend Radius = 15.278 in.

Column	Me kg/m	Rho kg/mee3	Veff m/sec	Vcrit m/sec	Veff/Vcrit
79	0.83363	142.974	2.763	3.606	0.766
80	0.83363	143.043	2.763	3.605	0.766
81	0.83370	143.295	2.778	3.602	0.771
84	0.83555	146.869	2.796	3.562	0.785
85	0.83682	149.468	2.809	3.534	0.795
86	0.83826	152.466	2.809	3.502	0.802

Statistics for row 14 with natural frequency 36.11 hz:

Average value of Veff/Vcrit = 0.781 over all tube columns processed
Maximum value of Veff/Vcrit = 0.802 occurs at tube column 86

through 1-6, column numbers which correspond to U-tubes not falling into the category described in NRC Bulletin 88-02 have been omitted for the sake of clarity. That is, entries appear only for tubes that are not supported by AVB's and have ECT indications of tube denting at the uppermost tube support plate. If these conditions are met for a tube position in any of the four steam generators at Haddam Neck, a table entry is present for that tube column. In addition, if such a tube is plugged (in all steam generators which qualify it for the specified category), it is omitted from the tables. There are no data presented here for tube rows 15 and 16 simply because all tubes in these rows do not fall into the designated category. Recent ECT inspections have shown that most of the tubes in rows 15 and 16 are supported by AVB's, and those few that are not have no observable denting.

The data for susceptibility ratio presented in Tables 1-4, 1-5 and 1-6 show that the maximum value of V_{eff}/V_{crit} for all tube rows of interest lies between 0.80 and 0.88, and occurs consistently at the largest column number in each row. The location of the maximum value is predicted to occur near the periphery of the bundle, where velocities tend to be the highest. The latter effect is due to the reduced resistance of flow parallel to the tubes (as opposed to flow normal to the tubes), the secondary flow tending to "skirt" around the tube bundle. Some of the higher values of susceptibility ratio are also found at the lowest column numbers (e.g., column 51), near the vertical plane of symmetry.

An assessment of the likelihood of a fluidelastic instability for susceptibility ratios of magnitude 0.88 can be made by comparing with similar data predicted for North Anna in the vicinity of the failed tube. Generally, experimental data implies that the onset of instability occurs when V_{eff}/V_{crit} exceeds 1.0.

1.4.2 Model 51

A fluidelastic instability analysis was performed for tube rows 7 through 11 of the Model 51 of North Anna, employing the resultant cross-flow tube gap velocity and a value of $\zeta = 0.017$ for the total damping ratio. Since denting data, AVB support status, and plugging information was lacking, we examined and reported results for each column of each row indicated.

The effective velocities, critical velocities and ratios V_{eff}/V_{crit} for the North Anna analysis are presented in Tables 1-7 through 1-11, corresponding to tube rows 7 through 11, respectively. Of particular interest, of course, is the value of susceptibility ratio in the immediate vicinity of the failed tube row 9 column 51 (R9C51) of North Anna. Due to the finite spatial resolution of the ATHOS3 calculation, and the inability of any existing thermal-hydraulic code to predict the exact profiles of void and velocity in the U-bend region, we do not anticipate that the model will be able to single out the exact location of the failed tube. Since our resolution is of the order of three tube pitches even with 11,000 cells, interpolation (presently, linear in three dimensions) must be employed to make evaluations for each distinct tube position in the bundle. With regard to the accuracy of the code prediction at a given computational node, comparisons with measured data from the CLOTAIRE experiments have shown that while ATHOS3 can capture the average value of a radial profile of void or velocity, typically, it can reproduce only the general shape of the profile (e.g., local differences may be of magnitude 5-10%). This also seems to be the case for other steam generator codes - THIRST, CAFCA, FIT and PORTHOS. Hence, it is important to interpret the results in the proper perspective.

Indeed, Table 1-9 shows that the value of susceptibility ratio calculated for R9C51 is S = 0.852, a value in the range of the maximum predicted for the Model 27. However, a higher value of S = 0.956 is found only three columns away, within the spatial resolution of the model, at the innermost column of row 9, column 48. A predicted value of V_{eff}/V_{crit} as large as 1.210 prevails at the outermost column of row 9, column 93. Of course, some of the tubes evaluated for the Model 51 might not fall into the category of interest, e.g., they may be plugged, undented, or supported by AVB's.

Table 1-10 shows that at column 51 of row 10, only a single pitch away from the failed North Anna tube, the susceptibility ratio is 0.998, essentially, the conventionally accepted value for the onset of instability, 1.0. Larger values of S are also found for the innermost and outermost tube columns of row 10, e.g., columns 48 through 50 and 90 through 93. The maximum value of susceptibility ratio for row 10 is S = 1.464, which occurs at outermost tube column 93. The average value of S for all columns of row 10 is close to 1.0, at S = 0.946. Several tubes of row 10 of the Model 51 at North Anna appear to be close to instability if they are indeed unsupported by AVB's and are also dented at the uppermost support plate.

As the bend radius increases, the natural frequency decreases and the critical velocity is reduced. Table 1-11, applicable to row 11, shows higher susceptibility ratios, with the average and maximum values of S being 1.098 and 1.756, respectively. The value of S at column 51 is 1.163, higher than that for rows 9 and 10. It may be true, of course, that the majority of tube columns of

Table 1-7. Westinghouse Model 51 Steam Generator (Thermal-Hydraulic Analysis With No AVB's Present).

Fluidelastic Instability Analysis of Row 7, Bend Radius = 9.876 in.

Column	Me kg/m	Rho kg/m**3	Veff m/sec	Vcrit m/sec	Veff/Vcrit
48	0.97941	162.289	5.309	8.093	0.656
49	0.97561	155.281	4.994	8.257	0.605
50	0.97387	151.813	4.869	8.344	0.576
51	0.97346	150.767	4.926	8.371	0.588
52	0.97374	151.020	5.110	8.365	0.611
53	0.97396	151.215	5.228	8.360	0.626
54	0.97412	151.355	5.170	8.357	0.619
55	0.97425	151.474	5.029	8.355	0.602
56	0.97429	151.445	4.846	8.356	0.580
57	0.97426	151.331	4.670	8.359	0.559
58	0.97412	151.045	4.453	8.366	0.532
59	0.97376	150.406	4.145	8.382	0.494
60	0.97415	151.039	4.104	8.366	0.491
61	0.97467	151.891	4.130	8.345	0.495
62	0.97520	152.765	4.159	8.323	0.500
63	0.97572	153.641	4.195	8.302	0.505
64	0.97628	154.591	4.237	8.279	0.512
65	0.97704	155.834	4.245	8.249	0.515
66	0.97847	158.172	4.287	8.194	0.523
67	0.97998	160.648	4.304	8.136	0.529
68	0.98156	163.252	4.349	8.078	0.538
69	0.98314	165.867	4.405	8.020	0.549
70	0.98405	167.342	4.403	7.989	0.551
71	0.98436	167.869	4.286	7.979	0.537
72	0.98467	168.268	4.164	7.969	0.523
73	0.98494	168.691	4.034	7.960	0.507
74	0.98517	169.045	3.943	7.953	0.496
75	0.98546	169.523	3.953	7.943	0.499
76	0.98573	169.952	3.985	7.934	0.502
77	0.98612	170.608	4.019	7.920	0.507
78	0.98700	172.073	4.082	7.890	0.517
79	0.98788	173.417	4.128	7.862	0.525
80	0.98909	175.558	4.168	7.819	0.533
81	0.99062	178.115	4.265	7.769	0.549
82	0.99290	181.878	4.373	7.697	0.568
83	0.99544	186.083	4.521	7.619	0.593
84	0.99727	189.129	4.619	7.565	0.597
85	0.99911	192.189	4.614	7.511	0.601
86	0.99997	193.600	4.439	7.487	0.593
87	1.00007	193.742	4.272	7.485	0.571
88	1.00013	193.807	4.101	7.483	0.548
89	1.00220	197.261	4.101	7.426	0.552
90	1.00747	206.014	4.459	7.285	0.612
91	1.01273	214.772	4.793	7.154	0.670
92	1.01799	223.524	5.117	7.030	0.728
93	1.02304	231.931	5.449	6.919	0.788
94	1.02362	232.884	5.466	6.907	0.791

Statistics for row 7 with natural frequency 96.59 hz:

Average value of Veff/Vcrit = 0.567 over all tube columns processed
Maximum value of Veff/Vcrit = 0.791 occurs at tube column 94

Table 1-8. Westinghouse Model 51 Steam Generator (Thermal-Hydraulic Analysis With No AVB's Present).

Fluidelastic Instability Analysis of Row 8, Bend Radius = 11.157 in.

Column	Me kg/m	Rho kg/m**3	Veff m/sec	Vcrit m/sec	Veff/Vcrit
48	0.97857	160.977	5.298	6.632	0.799
49	0.97513	154.655	5.041	6.754	0.746
50	0.97329	151.674	4.782	6.828	0.700
51	0.97293	150.110	4.876	6.848	0.712
52	0.97314	150.235	5.002	6.846	0.731
53	0.97335	150.420	5.075	6.843	0.742
54	0.97350	150.538	5.098	6.840	0.745
55	0.97355	150.506	4.969	6.841	0.726
56	0.97353	150.397	4.791	6.844	0.700
57	0.97339	150.095	4.578	6.850	0.668
58	0.97314	149.628	4.363	6.866	0.636
59	0.97278	148.984	4.064	6.873	0.594
60	0.97319	149.631	4.044	6.860	0.590
61	0.97371	150.473	4.062	6.843	0.594
62	0.97425	151.359	4.092	6.824	0.600
63	0.97478	152.245	4.116	6.806	0.605
64	0.97536	153.217	4.154	6.787	0.612
65	0.97609	154.418	4.169	6.763	0.616
66	0.97743	156.597	4.193	6.720	0.624
67	0.97882	158.874	4.222	6.677	0.632
68	0.98026	161.255	4.263	6.632	0.643
69	0.98172	163.675	4.314	6.588	0.655
70	0.98262	165.119	4.313	6.562	0.657
71	0.98299	165.671	4.211	6.552	0.643
72	0.98332	166.169	4.103	6.544	0.627
73	0.98366	166.691	3.991	6.534	0.611
74	0.98393	167.117	3.908	6.527	0.599
75	0.98423	167.598	3.926	6.519	0.602
76	0.98451	168.064	3.949	6.510	0.607
77	0.98497	168.825	3.989	6.497	0.614
78	0.98587	170.324	4.060	6.472	0.627
79	0.98669	171.682	4.115	6.449	0.638
80	0.98785	173.610	4.184	6.416	0.644
81	0.98928	175.990	4.214	6.378	0.661
82	0.99154	179.721	4.319	6.318	0.684
83	0.99484	183.859	4.474	6.255	0.715
84	0.99578	186.740	4.455	6.212	0.717
85	0.99754	189.651	4.432	6.169	0.718
86	0.99849	191.217	4.369	6.147	0.711
87	0.99877	191.650	4.232	6.141	0.689
88	0.99900	192.014	4.091	6.136	0.667
89	1.00138	195.968	4.128	6.081	0.679
90	1.00878	204.950	4.513	5.962	0.757
91	1.01218	213.935	4.871	5.851	0.832
92	1.01758	222.923	5.219	5.747	0.908
93	1.02285	231.345	5.572	5.656	0.985

Statistics for row 8 with natural frequency 78.87 hz:

Average value of Veff/Vcrit = 0.686 over all tube columns processed
Maximum value of Veff/Vcrit = 0.985 occurs at tube column 93

Table 1-9. Westinghouse Model 51 Steam Generator (Thermal-Hydraulic Analysis With No AVB's Present).

Fluidelastic Instability Analysis of Row 9, Bend Radius = 12.438 in.

Column	Me kg/m	Rho kg/m**3	Veff m/sec	Vcrit m/sec	Veff/Vcrit
48	0.97793	159.968	5.289	5.533	0.956
49	0.97480	154.263	5.056	5.625	0.899
50	0.97285	150.502	4.885	5.688	0.845
51	0.97245	149.505	4.861	5.707	0.852
52	0.97255	149.455	4.943	5.708	0.866
53	0.97271	149.555	4.928	5.707	0.863
54	0.97284	149.623	4.977	5.706	0.872
55	0.97289	149.612	4.918	5.706	0.862
56	0.97282	149.418	4.741	5.710	0.830
57	0.97265	149.065	4.535	5.716	0.793
58	0.97233	148.479	4.290	5.726	0.749
59	0.97191	147.752	4.011	5.739	0.699
60	0.97232	148.388	3.986	5.728	0.696
61	0.97282	149.181	4.004	5.714	0.701
62	0.97333	150.015	4.031	5.700	0.707
63	0.97386	150.915	4.057	5.684	0.714
64	0.97444	151.884	4.098	5.668	0.723
65	0.97513	153.005	4.098	5.649	0.725
66	0.97642	155.102	4.126	5.614	0.735
67	0.97778	157.318	4.156	5.579	0.745
68	0.97916	159.583	4.201	5.543	0.758
69	0.98052	161.815	4.238	5.508	0.769
70	0.98138	163.186	4.235	5.488	0.772
71	0.98176	163.760	4.145	5.479	0.757
72	0.98212	164.326	4.049	5.471	0.740
73	0.98250	164.911	3.952	5.462	0.724
74	0.98280	165.376	3.880	5.455	0.711
75	0.98311	165.870	3.892	5.448	0.714
76	0.98339	166.333	3.912	5.441	0.719
77	0.98385	167.108	3.955	5.430	0.728
78	0.98477	168.628	4.031	5.408	0.745
79	0.98568	170.001	4.091	5.388	0.759
80	0.98669	171.805	4.090	5.363	0.763
81	0.98803	174.036	4.142	5.332	0.777
82	0.99020	177.605	4.266	5.284	0.807
83	0.99256	181.495	4.434	5.233	0.847
84	0.99425	184.282	4.463	5.198	0.847
85	0.99598	187.146	4.361	5.162	0.845
86	0.99704	188.889	4.307	5.141	0.838
87	0.99749	189.617	4.195	5.132	0.817
88	0.99792	190.312	4.079	5.124	0.796
89	1.00060	194.769	4.156	5.072	0.819
90	1.00615	203.987	4.568	4.970	0.919
91	1.01171	213.226	4.950	4.874	1.015
92	1.01726	222.458	5.324	4.785	1.113
93	1.02232	230.862	5.696	4.709	1.210

Statistics for row 9 with natural frequency 65.61 hz:

Average value of Veff/Vcrit = 0.807 over all tube columns processed
Maximum value of Veff/Vcrit = 1.210 occurs at tube column 93

Table 1-10. Westinghouse Model 51 Steam Generator (Thermal-Hydraulic Analysis With No AVB's Present).

Fluidelastic Instability Analysis of Row 10, Bend Radius = 13.719 in.

Column	Me kg/m	Rho kg/m**3	Veff m/sec	Vcrit m/sec	Veff/Vcrit
48	0.97730	158.986	5.200	4.687	1.120
49	0.97444	153.794	5.073	4.759	1.066
50	0.97244	150.084	4.839	4.812	1.006
51	0.97200	148.968	4.820	4.829	0.998
52	0.97212	148.928	4.888	4.830	1.012
53	0.97221	148.918	4.841	4.830	1.002
54	0.97230	148.925	4.840	4.830	1.002
55	0.97230	148.824	4.813	4.832	0.996
56	0.97222	148.603	4.689	4.835	0.970
57	0.97201	148.199	4.478	4.842	0.925
58	0.97167	147.570	4.241	4.851	0.874
59	0.97122	146.814	3.947	4.862	0.812
60	0.97162	147.423	3.920	4.853	0.808
61	0.97210	148.188	3.943	4.842	0.814
62	0.97258	148.970	3.963	4.830	0.820
63	0.97309	149.820	3.995	4.818	0.829
64	0.97366	150.762	4.030	4.804	0.839
65	0.97433	151.869	4.045	4.788	0.845
66	0.97555	153.830	4.061	4.761	0.853
67	0.97684	155.935	4.093	4.732	0.865
68	0.97820	158.143	4.136	4.702	0.880
69	0.97954	160.329	4.164	4.673	0.891
70	0.98036	161.640	4.166	4.656	0.895
71	0.98072	162.190	4.082	4.649	0.878
72	0.98111	162.787	4.003	4.641	0.862
73	0.98153	163.448	3.926	4.633	0.847
74	0.98183	163.919	3.853	4.627	0.833
75	0.98219	164.483	3.867	4.620	0.837
76	0.98250	164.986	3.888	4.613	0.842
77	0.98296	165.743	3.926	4.604	0.853
78	0.98383	167.192	4.005	4.586	0.873
79	0.98463	168.520	4.071	4.570	0.891
80	0.98572	170.315	4.064	4.548	0.894
81	0.98703	172.497	4.103	4.522	0.907
82	0.98905	175.794	4.225	4.484	0.942
83	0.99122	179.355	4.395	4.444	0.989
84	0.99284	182.019	4.361	4.415	0.988
85	0.99456	184.858	4.309	4.385	0.983
86	0.99572	186.766	4.266	4.365	0.976
87	0.99632	187.742	4.183	4.355	0.956
88	0.99694	188.773	4.070	4.344	0.937
89	0.99990	193.707	4.188	4.295	0.975
90	1.00559	203.149	4.631	4.206	1.101
91	1.01129	212.608	5.039	4.123	1.222
92	1.01699	222.079	5.448	4.046	1.346
93	1.02260	230.392	5.830	3.982	1.464

Statistics for row 10 with natural frequency 55.43 hz:

Average value of Veff/Vcrit = 0.946 over all tube columns processed
Maximum value of Veff/Vcrit = 1.464 occurs at tube column 93

Table 1-11. Westinghouse Model 51 Steam Generator (Thermal-Hydraulic Analysis With No AVB's Present).

Fluidelastic Instability Analysis of Row 11, Bend Radius = 15.000 in.

Column	Me kg/m	Rho kg/m**3	Veff m/sec	Vcrit m/sec	Veff/Vcrit
48	0.97688	158.630	5.280	4.022	1.313
49	0.97407	153.308	5.104	4.078	1.251
50	0.97213	149.742	4.980	4.123	1.189
51	0.97157	148.459	4.813	4.139	1.163
52	0.97167	148.385	4.872	4.140	1.177
53	0.97174	148.318	4.790	4.141	1.156
54	0.97177	148.242	4.706	4.143	1.136
55	0.97176	148.125	4.692	4.144	1.132
56	0.97164	147.838	4.681	4.148	1.109
57	0.97140	147.381	4.423	4.154	1.065
58	0.97106	146.759	4.192	4.162	1.007
59	0.97058	145.951	3.915	4.172	0.938
60	0.97064	146.495	3.874	4.165	0.930
61	0.97143	147.279	3.899	4.155	0.938
62	0.97194	148.096	3.930	4.145	0.948
63	0.97241	148.882	3.952	4.135	0.956
64	0.97294	149.760	3.985	4.124	0.966
65	0.97354	150.745	3.999	4.112	0.973
66	0.97471	152.623	4.014	4.089	0.982
67	0.97595	154.621	4.047	4.065	0.996
68	0.97724	156.725	4.083	4.040	1.011
69	0.97853	158.812	4.118	4.016	1.025
70	0.97937	160.144	4.120	4.001	1.030
71	0.97978	160.782	4.050	3.994	1.014
72	0.98013	161.301	3.988	3.988	0.995
73	0.98053	161.938	3.900	3.981	0.980
74	0.98091	162.536	3.848	3.975	0.968
75	0.98129	163.131	3.849	3.968	0.970
76	0.98163	163.682	3.859	3.962	0.974
77	0.98210	164.452	3.912	3.954	0.989
78	0.98293	165.822	4.007	3.939	1.017
79	0.98368	167.067	4.062	3.926	1.035
80	0.98474	168.820	4.050	3.908	1.036
81	0.98600	170.895	4.079	3.888	1.050
82	0.98791	174.008	4.198	3.855	1.089
83	0.98996	177.356	4.355	3.823	1.139
84	0.99157	179.988	4.321	3.798	1.138
85	0.99331	182.853	4.272	3.771	1.133
86	0.99453	184.871	4.231	3.753	1.128
87	0.99524	186.042	4.148	3.742	1.108
88	0.99607	187.419	4.078	3.730	1.093
89	0.99930	192.802	4.237	3.684	1.150
90	1.00513	202.464	4.709	3.606	1.306
91	1.01096	212.145	5.146	3.532	1.457
92	1.01679	221.824	5.580	3.464	1.611
93	1.02172	229.998	5.988	3.410	1.756

Statistics for row 11 with natural frequency 47.44 hz:

Average value of Veff/Vcrit = 1.098 over all tube columns processed
Maximum value of Veff/Vcrit = 1.756 occurs at tube column 93

row 11 are supported by AVB's, which is a design criterion for the Model 51.

A comparison of critical velocities for the Model 27 and Model 51 for a tube of the same bend radius (compare Table 1-4 with Table 1-8) shows that the values of V_{crit} for the Model 51 are generally higher. This is due primarily to the larger tube diameter for the Model 51 (0.875 in. vs. 0.750 in.), as noted earlier. The susceptibility ratios for a Model 51 tube of equivalent bend radius are higher, despite the larger values of V_{crit}, since the effective velocities appear to be higher than in the Model 27. In the case of rows 7 and 8 of the Model 51, the critical velocities are generally large enough to rule out an instability, as Tables 1-7 and 1-8 indicate.

1.5 SUMMARY

The U-tubes of inner rows of the Westinghouse Model 27 and Model 51 steam generators have been evaluated for fluidelastic instability. The objective was to provide an assessment of stability for the Model 27 at Haddam Neck, in light of qualifying the JAYCOR model with a known failed tube at North Anna 1. The focus of the study was on U-tubes which are unsupported by AVB's and have observed denting at the uppermost tube support plate. While the Model 27 thermal-hydraulic simulation accounted for the presence of AVB's of nonuniform elevations, the Model 51 calculation assumed no flow blockages due to anti vibration bars. Hence, the Model 27 analysis at least partially accounted for flow peaking effects due to anti-vibration bars (only partially, due to practical limits of spatial resolution). The fluidelastic instability analyses made use of empirical damping coefficients obtained from recent two-phase flow steam-water experiments [6]. The influence of void fraction on total damping was taken into account in the analyses of the Model 27 and Model 51. The resultant of the in-plane and out-of-plane cross-flow tube gap velocity components were employed in both analyses. Values of susceptibility ratios of inner rows of each steam generator are reported and compared.

1.6 CONCLUSIONS

An analysis of the Model 27 steam generator at Haddam Neck reveals that the maximum values of V_{eff}/V_{crit} for rows 10, 11 and 12 are 0.878, 0.872 and 0.862, respectively, for all tubes which are not supported by AVB's, are dented at the uppermost support plate, and are not plugged. Hence, the largest susceptibility ratio, S = 0.878, is below the critical limit of 1.0 for all tubes of interest relative to NRC Bulletin 88-02. Maximum values of V_{eff}/V_{crit} are predicted near the wrapper wall, where the secondary flow tends to skirt around the tube bundle, seeking the lowest path of resistance.

A measure of the likelihood of a fluidelastic instability at Haddam Neck has been ascertained by comparing the results for the Model 27 with similar data predicted by the same method, for a known failed tube of the Model 51 steam generator at North Anna 1. Our analysis has shown that relative to the spatial resolution and practical accuracy of the thermal-hydraulic ATHOS3 calculation, instability is predicted in the immediate vicinity of the failed tube R9C51. The spatial resolution of the ATHOS3 finite-difference grid is about three tube pitches in the U-bend

region. Although the predicted value of susceptibility ratio is 0.852 at tube location R9C51, we find that S = 0.998 for row 10 column 51, a tube which is an immediate neighbor of R9C51. The maximum value of V_{eff}/V_{crit} for row 10 occurs at the outermost column, near the wrapper wall, and is relatively large at 1.464. In the same row as the failed tube, but three columns away, we find that S = 0.956. At the same column number as the failed tube, we have S = 1.163 in row 11, two tube pitches away from R9C51.

Hence, we conclude that our model for evaluating fluidelastic instability is consistent with the North Anna 1 tube failure, within the practical limits of spatial resolution of the thermal-hydraulic simulation. It appears that a reasonable critical value of susceptibility ratio applicable to our model is close to 1.0, which implies that we have selected reasonable values of empirical parameters such as the total damping ratio.

Susceptibility ratios which are more than 12% below the critical limit for stability are predicted for the Model 27 steam generator at Haddam Neck. In light of our conservatively-based approach (e.g., selection of a circulation ratio in the high end of the accepted range for the Model 27), we conclude that fluidelastic instability is unlikely to occur for this unit. Certainly, any flow peaking effect present in the North Anna 1 configuration would widen the difference between the critical limit we have determined and the susceptibility ratios calculated for the Model 27. This is indeed the case, since we have partially accounted for flow peaking in the Model 27 calculation, and have not in the Model 51 analysis. Flow peaking effects would tend to increase the values of susceptibility ratios determined for the North Anna 1 evaluation.

2. Response to NRC Item 2: ATHOS Slip Model

> "Why does ATHOS code give slip (unequal phase velocities) in axial direction only?"

During the early development and testing of the ATHOS code, it was determined that convergence was difficult to achieve with the "general slip" option, that is, where slip was allowed in all coordinate directions. This may have been partly due to discontinuities in interphase friction correlations at the extremes of differing flow regimes. It was then decided that it was best to offer an "algebraic slip" option, where slip is allowed only in the predominant flow direction in a steam generator, the axial direction. With this model, the relative velocity between the vapor phase and the mixture is deduced from a drift-flux formulation, while the mixture velocity is calculated from a mixture momentum equation. The present alternative in ATHOS is the homogeneous option, where phasic velocities are equal in all coordinate directions.

3. Response to NRC Item 3: K-Loss Factors

The design analysis sheets for calculation of K-loss factors are attached as Appendix A.

4. Response to NRC Item 4: Translational and Rotational Stiffnesses

The translational and rotational stiffnesses identified in the 1986 study by Schoof [7] have been deduced from experimental results for a scale model steam generator. The experiment was part of the Degraded Tube Support Evaluation Program, of which ANL was a participant. Please refer to Section 2.5 of Reference 7.

5. Response to NRC Item 5: Selection of Total Damping Ratio

We have attached a copy of the paper,

> M. J. Pettigrew, L. N. Carlucci, C. E. Taylor and N. J. Fisher, "Flow-Induced Vibration and Related Technologies in Nuclear Components," ASME PVP Conference, April 1989.

which is Reference 7 of the JAYCOR report [1].

The value of total damping ratio of 0.03 was inferred from Figure 14 of the Pettigrew, et al. paper, which we present here as Figure 5-1. The experimental data for a normal square pitch (square symbols) were used in conjunction with an average void fraction for the entire U-bend region of 0.88. Figure 5-1 applies to damping measurements in air-water mixtures with confinement ratios of P/D=1.47.

We have reviewed the reference mentioned in NRC Item 5,

> Axisa, et. al., "Vibration of Tube Bundles Subjected to Air-Water and Steam-Water Crossflow: Preliminary Results on Fluidelastic Instability," Symposium on Flow-Induced Vibration, Vol. 2, pgs. 269-284, 1984.

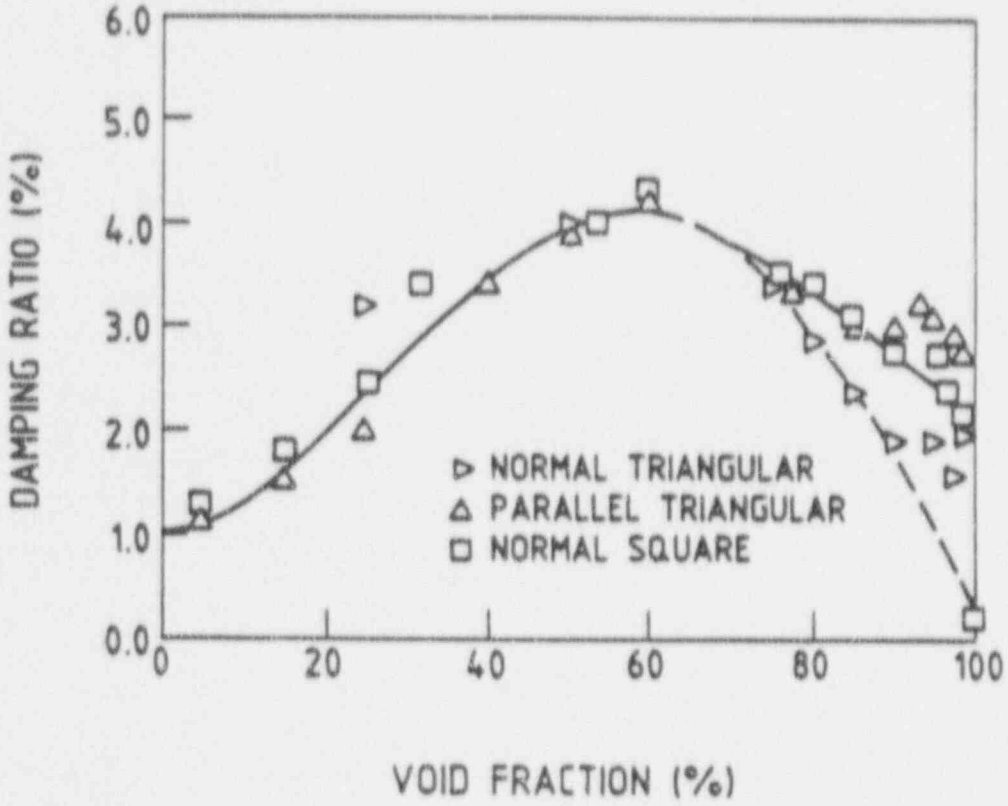

Figure 5-1. Damping for tube bundles of P/d = 1.47 in air-water mixtures. Solid curve is average damping for the three bundle configurations. Dashed curve is an approximation of damping without the effect of intermittent two-phase flow. Reprinted from Reference 3, Pettigrew, Carlucci, Taylor and Fisher.

and have found that Axisa has since published a paper where he has "revisited" his earlier calculations of damping,

> F. Axisa, M. Wullschleger, B. Villard and C. Taylor, "Two-Phase Cross-Flow Damping in Tube Arrays, ASME-PVT Vol. 133. Presented at ASME-PVP Conference, Pittsburgh, June 1988.

In this paper, Axisa presents results of an improved method for obtaining damping coefficients from measured spectra. A subsequent paper by Pettigrew, et al., includes the revisited Axisa data in a comprehensive collection of damping data for single phase and two-phase flow conditions,

> M. J. Pettigrew, C. E. Taylor and B. S. Kim, "Vibration of Tube Bundles in Two-Phase Cross-Flow: Part 1 -Hydrodynamic Mass and Damping," ASME-PVT Vol. 111, November 1989. Presented at 1988 International Symposium on Flow-Induced Vibration and Noise, ASME WAM, PVP Division, Volume 2, Chicago, Nov. 27-Dec. 2, 1988.

This paper is Reference 2 of the current report. Note that Figure 5-1 also appears as Figure 15 in Reference 2.

We have recently conducted a literature survey including over 50 references pertinent to flow induced vibration (FIV). Although much work has been done in the last decade, there is still an apparent scarcity of data on damping in two-phase flow, particularly in steam-water. It does appear that damping ratios obtained in steam-water are generally lower than in air-water, the latter configuration being by far the most common experimental test base. Pettigrew [2] and Axisa [6] have both suggested that the lower damping values may be attributable to the lower surface tension in steam-water mixtures than in air-water.

The magnitude of total damping in two-phase flow depends on several parameters [2], e.g., void fraction, flow regime, hydrodynamic mass/cylinder mass. Damping has also been shown to have a finite but weak dependence on frequency, confinement (pitch-to-diameter ratio) and mass flux. Since damping in two-phase flow appears to have the strongest dependence on void fraction, we have chosen to account for this effect in all of our fluidelastic instability analyses. In our recent evaluations for the Model 27 and Model 51 steam generators, we have calculated the average void fraction in the three-dimensional space occupied by the tube rows of interest in the U-bend region. We then inferred a value of total damping ratio from the curve for steam-water in Figure 1-1 (Figure 17 of Reference 2), applicable to the most recently published Axisa data (1988). The same procedure and the same damping vs. void fraction curve were employed for both the Model 27 and the Model 51 analyses. The measured data for damping in steam-water have as their source the EVA experiments conducted by the CEA in France during the early-mid 1980's.

6. Response to NRC Item 6: Velocity Components in U-Bend

The selection of a suitable effective velocity in the U-bend region is not very straightforward. With regard to the effective velocity, it is not really clear that the same general rules which apply to the straight tube section also apply to the curved tubes in the U-bend. For example, is weighting the square of the velocity with the square of the displacement also valid for the U-bend region? A further complication is that there are separate phasic velocities in the axial direction available from the thermal-hydraulic calculation (with the algebraic slip option in force). The standard practice is to employ a mixture velocity, which we have done here. Of course, the fluid velocity obtained from the code (actually, an "approach" velocity into a cell) must be converted into a tube gap velocity. Finally, the velocity at a node along the tube must be determined from values at cell edges, by means of interpolatio three-dimensional space.

What we can be assured of in the present study is that the method used for the determination of effective velocity for the Model 27 at Haddam Neck is the same as it is for the Model 51 at North Anna.

In accordance with the recommendation of the NRC, we have taken into account both the in-plane and out-of-plane cross-flow velocities in our recent evaluations for the Model 27 and Model 51. Specifically, we have employed the magnitude of the resultant vector formed by component velocity vectors in the plane of the tube, and normal to the plane of the tube. The component vectors are each normal to the U-tube, and each give rise to a cross-flow condition. Hence, velocity components U_{gap}, V_{gap} and W_{gap} in all coordinate directions, θ, r, and z, respectively, are included in the determination of effective velocity.

7. Discussion

The present report provides the NRC with detailed responses to their request for additional information in connection with fulfilling requirements of NRC Bulletin 88-02. A technical approach for the assessment of the likelihood of a fluidelastic instability has been qualified with North Anna 1 data upon the recommendation of the NRC, and the results have been reported in Section 1. It has been found that the JAYCOR model does indeed result in a prediction of susceptibility ratios (effective velocities divided by critical velocities) greater than 1.0, within a distance of the failed tube (R9C51) not exceeding the spatial resolution of the thermal-hydraulic simulation. The analysis of North Anna 1 indicates that for a location which is a single pitch away from R9C51, at column 51 of row 10, the susceptibility ratio is essentially 1.0, at S = 0.998. Further evidence is shown by the maximum predicted values of susceptibility ratio for rows 9, 10 and 11, all well above the conventional critical value of S = 1.0, at S = 1.210, 1.464 and 1.756, respectively. These results for a scenario with a known failed tube should lend credibility to the integrity of the overall technical approach.

Subsequent to the time at which a draft copy of this report was submitted to the NRC for their review, a joint NRC/NUSCO/JAYCOR conference call was made [9], during which several concerns of the NRC were brought forth. We now take the opportunity to respond to these concerns, in the separate discussions which follow.

7.1 RELIABILITY OF INPUT DATA EMPLOYED FOR NORTH ANNA 1 ANALYSIS

There was some apparent concern by the NRC with regard to the principal investigator not being supplied with operational and geometric data for North Anna 1 directly from Virginia Power Company (VEPCO) or Westinghouse. A request was made to incorporate into the final report a table of operational data employed in our analysis. This has been done, and Table 1-1 has been added to Section 1. In addition, Table 1-2 describes the geometric specifications assumed for the Westinghouse Model 51 at North Anna 1. All of the input data used in our analysis have been obtained from three sources: (1) work we have performed for the Electric Power Research Institute (EPRI) over the last decade, (2) data we have accumulated during the course of consulting agreements and joint projects we have had with Westinghouse over the last several years, and (3) information available in the public domain.

7.2 ANTI-VIBRATION BARS NOT MODELED IN NORTH ANNA 1 ANALYSIS

Since we were lacking data for the individual penetration depths of anti-vibration bars for North Anna 1, we did not incorporate the AVB's into the geometric description of the Westinghouse Model 51. Hence, we accept that we did not account for flow peaking factors in the North Anna 1 evaluation. Flow peaking effects would tend to increase the predicted susceptibility ratios due

to local increases in effective velocities (V_{eff}), although the increase might not be as large as anticipated because of the practice of weighting along the length of a U-tube (see Equation 6-1 of Ref. 1) in the determination of V_{eff}. In any case, as pointed out in Section 1.6, accounting for flow peaking effects in the North Anna 1 analysis would tend to widen the differences between the susceptibility ratios calculated for Haddam Neck and North Anna, thus yielding a wider safety margin with respect to the likelihood of a fluidelastic instability occurring at Haddam Neck.

7.3 MARGIN BETWEEN SUSCEPTIBILITY RATIOS FOR HADDAM NECK AND NORTH ANNA

A concern of the NRC is whether the margin between the maximum susceptibility ratios for Haddam Neck and North Anna is large enough. The maximum predicted value of S for the Westinghouse Model 27 steam generators at Haddam Neck is S = 0.88, compared with S = 0.998 for a tube a single pitch away from the failed tube at North Anna 1. Maximum calculated values of S for all columns of rows at and near R9C51 of North Anna are as large as 1.756, however. It should be emphasized that the present state-of-the-art is such that it is not possible to predict the exact location of a potentially troublesome tube, and the best one can hope to do is to reveal the approximate location in the tube bundle (e.g., identification of a potentially unsafe row, or prediction of the location of a suspect tube to within several tube pitches). There is also, of course, a fair degree of uncertainty in experiments designed to obtain sensible values of susceptibility ratios, due to similarity assumptions and other factors.

It should be pointed out that the Westinghouse Model 27 analysis for Haddam Neck can be said to be conservatively-based. One reason why we feel that this is an acceptable statement, is that we have selected to employ a circulation ratio (CR) which is at the high end of the design range. The design value of CR is usually determined by the vendor using a 1-D model, based on measured or estimated K-losses for devices such as the steam separator, tube support plates, and downcomer. Our data base on the Westinghouse Model 27 includes design values of circulation ratio in the range $3.8 < CR < 4.8$. We have chosen to accept the value of CR = 4.54 predicted by ATHOS3 (employing nominal estimates for K- loss coefficients), although the circulation ratio might have a value as low as 3.8 in practice. It seems likely that due to the accumulation of deposits in the secondary flow passages through tube support plate gaps and flow holes over 24 years of operation at Haddam Neck, the circulation ratio might indeed be at the low end of the design range. A lower value of circulation ratio would result in lower axial velocities throughout the wrapper region, hence, lower effective velocities would be employed in the evaluation of fluidelastic instability.

7.4 NATURAL FREQUENCY OF NORTH ANNA TUBE R9C51

The NRC apparently feels that the natural frequency predicted by ADINA for the failed North Anna tube R9C51 is somewhat high at 65.6 Hz compared to a Westinghouse value of about 60 Hz. This implies that the value assumed for the length of the U-tube straight stub might not be

representative of the actual North Anna geometry. However, it should be pointed out that the effect of an overprediction of natural frequency would be an increase in the calculated value for critical velocity and a decrease in susceptibility ratios predicted for North Anna. If the value of natural frequency is lowered relative to our prediction of 65.6 Hz, this would widen the differences in susceptibility ratios between Haddam Neck and North Anna 1. For example, if we accept the value of natural frequency of 60 Hz for R9C51, all susceptibility ratios predicted for row 9 of North Anna 1 would be increased by 9.3%.

8. References

1. P. J. Masiello and P. F. Mlakar, "Fluidelastic Instability Analysis of the U-Bend Region of a Westinghouse Model 27 Steam Generator," JAYCOR Report J5439-89-001R1, Rev. 1, July 1989.

2. M. J. Pettigrew, C. E. Taylor and B. S. Kim, "Vibration of Tube Bundles in Two-Phase Cross-Flow: Part 1 - Hydrodynamic Mass and Damping," ASME-PVT Vol. 111, November 1989. Presented at 1988 International Symposium on Flow-Induced Vibration and Noise, ASME WAM, PVP Division, Volume 2, Chicago, Nov. 27-Dec. 2, 1988.

3. M. J. Pettigrew, L. N. Carlucci, C. E. Taylor and N. J. Fisher, "Flow-Induced Vibration and Related Technologies in Nuclear Components," ASME PVP Conference, April 1989.

4. M. J. Pettigrew and D. J. Gorman, "Vibration of Heat Exchanger Tube Bundles in Liquid and Two-Phase Cross-Flow," ASME PVP Volume 52, 1981.

5. M. J. Pettigrew, Y. Sylvestre and A. O. Campagna, "Vibration Analysis of Heat Exchanger and Steam Generator Designs," Nuclear Engineering and Design, Vol. 48, pp. 97-115, 1978.

6. F. Axisa, M. Wullschleger, B. Villard and C. Taylor, "Two-Phase Cross-Flow Damping in Tube Arrays, ASME-PVT Vol. 133. Presented at ASME-PVP Conference, Pittsburgh, June 1988.

7. C. C. Schoof, T. P. Khatua, L. M. Shusto, S. P. Winder and J. M. Thomas, "Millstone II Degraded Support Analysis: Analysis of Tube Vibrations and Tube-Support Interaction Forces," Failure Analysis Associates Report FaAA-R-85-04-02, December 1986.

8. Axisa, et al., "Vibration of Tube Bundles Subjected to Air-Water and Steam-Water Crossflow: Preliminary Results on Fluidelastic Instability," Symposium on Flow-Induced Vibration, Vol. 2, pgs. 269-284, 1984.

9. NRC/NUSCO/JAYCOR joint conference call, April 26, 1991, particpants include:

   NRC: E. Murphy, A. Wang
   NUSCO: S. Chandra, E. Perkins, G. Van Noordennen, L. Laskowski
   JAYCOR: P. Masiello

Appendix A

DESIGN ANALYSIS SHEETS FOR CALCULATION OF K-LOSS FACTORS

JAYCOR
DESIGN CALCULATION SHEET

(cover page)

Project Number: 5439-00

Originator: Paul J. Marcello

Checker:

Reason for calculation: Summarize tube support plate geometry and calculate loss coefficients for W Model 51 SG

Revision number: 0

PLEASE INDICATE SOURCE OF ALL INPUT DATA USED IN THE CALCULATION.

Data below from telephone conversation with Lenny Lastowski on 4-2-89:

Tube hole diameter = 0.764 in. $\equiv D_{TH}$

Flow hole diameter = 0.535 in. $\equiv D_{FH}$

Radius of tube support plate = R_w − 0.75 in $\equiv R_{TSP}$
where R_w = inner radius of wrapper wall
= 106.25 in/2 = 53.1250 in
↑ from Design Sheet 3-3-89, "Lay out geometry for establishing finite-difference grid"

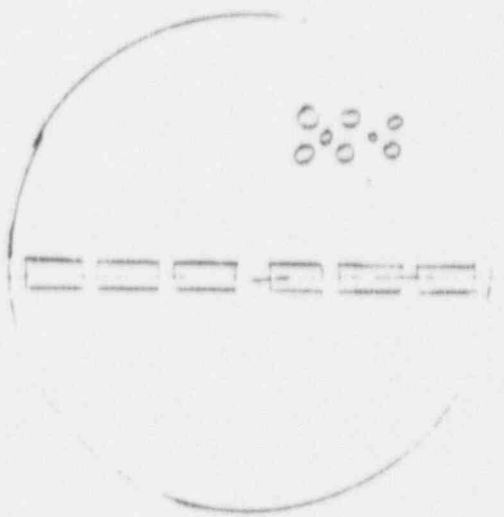

$A_{TSP_{geom}} = \pi R_{TSP}^2$ = 8766.409 in² = geometric area of a full tsp (no tube holes, etc.) ✓

$A_{HOLES} = 2[(3794)(\frac{\pi}{4} D_{TH}^2 + \frac{\pi}{4} D_{FH}^2)]$

$= 2[3794)\frac{\pi}{4}((0.764\,in)^2 + (0.535\,in)^2)] = 5184.252\ in^2$

$\Delta_d = \frac{\text{area occupied by restrictive device}}{\text{nominal area}} \equiv \text{AREMME} = \frac{A_{TSP_{geom}} - A_{HOLES}}{A_{TSP_{geom}}}$

$= \frac{8766.409\ in^2 - 5184.252\ in^2}{8766.409\ in^2} = 0.41528$ ✓

Note - Do not take into account flow slots since geometric AREMME will be used for a representative value across entire plate, not just those tubes with

Checker's initials P C
and date 5-17-1989

JAYCOR
DESIGN CALCULATION SHEET

(attachment page)

Rev. 0

Summarize tube support plate geometry and calculate loss coefficients for W 1 del 27 sa

Project Number: 5939-00
Originator: Paul T. Masiello
Checker:

Alternate method for computation of A_{REMME}, "mesh" area density ⇒
Consider a unit "cell" of one pitch by one pitch

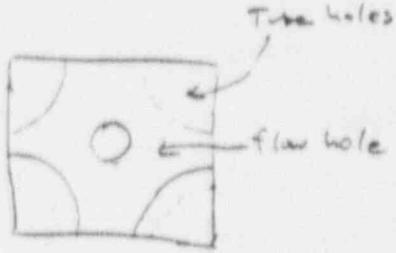

$$A_{REMME} = \frac{P^2 - \frac{\pi}{4}(D_{TH}^2 + D_{FH}^2)}{P^2} = \alpha_d$$

where P = tube pitch = 1.03125 in.

$$\text{So } A_{REMME} = \frac{(1.03125\,in)^2 - \frac{\pi}{4}\left((0.760\,in)^2 + (0.535\,in)^2\right)}{(1.03125\,in)^2}$$

$$= 0.35755 \checkmark$$

Use this value, since it is most representative - it prevails for area where tubes are.

Will base loss coefficient for the plate on this value. Ratio of device area (area free to flow) to approach area is

$$\sigma = \frac{A_d}{A_a} = \frac{P^2 - \alpha_d P^2 - A_T}{P^2 - A_T} = \frac{P^2(1-\alpha_d) - A_T}{P^2 - A_T}$$

where A_T = cross-sectional area of a tube (based on it's outer diameter) = $\frac{\pi}{4} D_o^2$, $D_o = 0.75$ in

$$\sigma = \frac{A_d}{A_a} = \frac{P^2(1-\alpha_d) - \frac{\pi}{4} D_o^2}{P^2 - \frac{\pi}{4} D_o^2} = 0.38837 \checkmark$$

$$\sqrt{\sigma} = \frac{A_a}{A_d} = 1/0.38837 = 2.57484 \checkmark$$

Loss coefficients for plate ⇒

$$K_{ATHOS} = \frac{K_a}{2}\left(\frac{A_d}{A_a}\right)^2 = \frac{K_a}{2}\sigma^2 \quad \text{where } K_a = \text{loss coefficient based on approach area}$$

Checker's initials PC
and date 5-17-1989

JAYCOR
DESIGN CALCULATION SHEET

Rev. 0

(attachment page)

Summarize tube support plate geometry and calculate loss coefficients for W model 79 SG

Project Number: 5439-00
Originator: Paul J. Musiello
Checker:

(1) $K_a = [0.4(1-\sigma^2)+(\sigma-1)^2]/\sigma^2$ From W work, Model D3, 9-9-82

$K_{ATHOS} = \frac{K_a}{2}\sigma^2 = \frac{1}{2}[0.4(1-\sigma^2)+(\sigma-1)^2] = 0.35688$ ✓

(2) $K_a = \frac{1.1}{\sigma^2}\left[(0.5+0.24\sqrt{1-\sigma})(1-\sigma)+(1-\sigma)^2\right]$ same source as (1)

$K_{ATHOS} = \frac{1.1}{2}[\quad] = 0.83709$ ✓

(3) $K_a = \frac{1}{2}\left(\frac{1}{\sigma}-1\right)^2$ ATHOS3 option for auto calc of K_a

$K_{ATHOS} = \sigma^2\left(\frac{1}{\sigma}-1\right)^2 = 0.18704$ seems low ✓

Will use relation (2), ∴ $K_{ATHOS} = 0.437 \equiv$ CLEGG ✓

Reason is - use higher value because magnetite deposits will reduce effective flow area

FLOW SLOTS NEAR TUBE LANE AREA -

From conversation with L Lestourgeon, NW, 4-3-79 flow slots on manway side (of interest here, contains high columns with flow tunneling due to AVB depths) have "hourglass" effect. They have actual widths of 2.1, 2.375 and 1.25 in. Nominal width is 2.375 in. Lastransit save length of 15½ in, and from range of tube columns traversed (2-17), (18-33), (34-49), would be (17-2)(1.0312.5in)
= 15.46875 in ✓

Approach - Will assume an effective gap between 2 and 17 of plate as if it were continuous, with no divisions / webs. The gap will have the same flow area as the measured, hourglassed, slots. The minimum widths are given. Assume an average width across each slot, and assume slot has nominal width at each end.

Checker's initials and date

JAYCOR
DESIGN CALCULATION SHEET

(attachment page)

Rev 0

Summarize tube support plate geometry and calculate loss coefficients for W model 27 SG

Project Number: 5439-00

Originator: Paul J. Mastrello

Checker:

Therefore, the average width of each slot in each quadrant is

$\frac{1}{2}(2.375\,in + 2.1\,in)$, $\frac{1}{2}(2.375\,in + 2.375\,in.)$, $\frac{1}{2}(2.375\,in + 1.76\,in)$

or 2.2375 in, 2.3750 in., 2.0675 in

Total slot flow area in this quadrant is then

$A_{eff} = (15.5\,in)(2.2375\,in + 2.3750\,in + 2.0675\,in) = 103.54\,in^2$

Neglect rounded corners of each slot, since we are dealing with an approximate average value anyway.

The wrapper radius is $R_w = 52.125\,in$ (see design sheet "Lay out geometry... 3-31-89). Then

$R_w \delta_{eff} = A_{eff}/2$ neglecting curvature at end of plate

where δ_{eff} = effective gap between R_w and plate

$$\delta_{eff} = \frac{A_{eff}}{2R_w} = \frac{103.54\,in^2}{2(52.125\,in)} = 0.9945\,in. \quad \text{(DSHPEC)}$$

Will model plates as "partial" tube support plates,

Checker's initials PC
and date 5-18-89

Docket No. 50-213
A08903
B13890

Attachment No. 2

Haddam Neck Plant

Steam Generator Top Tube Support Plate Denting

August 1991

I.E. Bulletin 88-02 Addendum

Connecticut Yankee Steam Generator

Top Tube Support Plate Denting

Tube support plate denting for the top tube support plate (tube support plate #4) on both the hot legs and cold legs of each steam generator were measured for each tube in rows 10 to 15 using SG eddy current test (ECT) data from the 1987 CY SG ECT inspection.

To allow some means of equating eddy current dent voltage response to dent size (a nominal 1 mil dent produces a 20 volt signal response), an in-line dent standard, used during the 1987 SG ECT inspection, was used during the ECT data review.

In general, most tube support plate lissajous signals in SG1 and SG2 were rotated. This indicates that general uniform tube support plate corrosion exists for the top tube support plates for SG1 and SG2. SG3 and SG4 have essentially no denting and no support plate signal rotations indicating that essentially no tube support plate corrosion exists for SG3 and SG4. Any signal which was rotated was classified as dented and in most cases showed some degree of denting. These tubes which had clear dent signals and/or rotated tube support plate signals were plotted on SG maps.

In addition to the 1987 ECT data review, a 100 percent dent reanalysis for all tube support elevations and intersections was performed on the 1987 and 1989 data to determine if changes had occurred since the 1987 SG ECT inspection. This review showed no changes and confirmed the initial 1987 ECT data review.

Docket No. 50-213
A08903
B13890

Attachment No. 3

Haddam Neck Plant

Plant Procedures:

SUR 5.1-2
AOP 3.2-31
ANN 4.20-9
AOP 3.2-2
SUR 5.4-44

August 1991